

Congestion Management for Cost-effective Power Grid Load Balancing using FACTS and Energy Storage Devices allocated via Grid Curvature Means

Edmond Jonckheere, Reza Banirazi and Eugenio Grippo

Abstract—A new method for congestion management is introduced based on a new concept of graph curvature. Fundamentally, a new curvature concept is presented and utilized to detect congestion within the power grid. From the premise that a negative curvature property means that the grid is prone to congestion in the sense that some lines carry a significant amount of power compared to the other lines, the congested lines are identified using a novel curvature-driven centrality measure. Once the congested areas/lines are identified, methods to control/mitigate congestion via curvature maximization are presented and revolve around the idea of deploying FACTS (Flexible Alternating Current Transmission System) devices and extra loads—storage elements—that drain the power overflow away from the congestion areas in such a way as to minimize the cost of energy production while maintaining stability via phase angle and voltage constraints. The same method also embodies control/mitigation of line loading relative to their thermal ratings, by incorporating constraints on the power flowing through the lines.

I. INTRODUCTION

One of the premises of the “smart grid” is to allow consumers to purchase electricity at the cheapest price, with the drawback that this creates large transfer of power across the grid with the potential to overload some lines in some unpredictable fashion resulting from the randomness of the renewables and electric vehicle charging. Line overloading is usually measured through a line utilization index that scales the apparent power by the thermal rating of the line. The absolute loading of the lines, that is, the apparent power carried by the lines irrespective of their thermal rating, depends on the generation supply, the consumer demand, and the topology of the grid. By “topology” of the grid, we mean the topology of the graph abstracting the bus system and the line susceptances and conductances.

The Congestion Management (CM) literature incorporates a wealth of strategies that aim to alleviate power grid congestion, such as, Generators Rescheduling (GR), load shedding, Distributed Generation (DG), Optimal Power Flow (OPF), Flexible Alternating Current Transmission System (FACTS) devices, Artificial Bee Colony algorithm (ABC), Genetic Algorithms (GA), Strength Pareto Evolutionary Algorithm (SPEA), just to name a few (see [1], [2], [3], [4], [5], [6] and [7] for a comprehensive review). This work proposes a method that combines FACTS (Sec. IV-A) and storage element deployment via curvature analysis leading to a new

grid shielding method that “reroutes” the power flow in a cost-conscious manner.

This method is embodied in a cost/curvature constrained power flow optimization method to prevent line overloading (Secs. IV, IV-C).

Towards the end of this work, the suggested procedure is equipped with constraints on the line utilization (active power scaled by line capacity) rather than the mere active power, further improving the overall method.

Simulation on the IEEE300 bus system shows effectiveness of the method, with some educated guess on the line capacity since the IEEE300 does not provide such data.

II. RESISTIVE NETWORK MODELS OF POWER FLOWS

Given two buses k and m specified by their voltage magnitude and phase angle pairs (V_k, θ_k) and (V_m, θ_m) , resp., connected by a transmission line with admittance $Y_{km} = G_{km} - jB_{km}$, the power flow equations, under the standard approximations of a nearly lossless lines ($G_{km} \approx 0$) with small phase angle differences ($\theta_k \approx \theta_m$), they are simplified to be

$$P_{km} = B_{km}V_kV_m(\theta_k - \theta_m), \quad Q_{km} = V_kB_{km}(V_k - V_m).$$

where P_{km} and Q_{km} are the active and reactive power, resp., flowing from bus k to bus m . Hence, P_{km} can be viewed as the current flowing through a resistor $\rho_{km} = 1/B_{km}V_kV_m$ driven by a voltage potential difference $\theta_k - \theta_m$. Active powers injected at some buses are then modeled as currents injected at the corresponding nodes of a resistive network. Let us call this resistive network the P -graph.

Similarly, Q_{km} can be viewed as the current flowing through a directional resistor $\rho_{km} = 1/B_{km}V_k$ driven by a voltage potential difference $V_k - V_m$. We refer to this directed resistive network as the Q -digraph.

While the P -graph and the Q -digraph allow for a quick snapshot of active and reactive power load, respectively, the apparent power carried by the line is $\sqrt{P_{km}^2 + Q_{km}^2}$, mandating some way to combine the two power flows [8]. Here we combine the two power flows in the way their fluctuations, resulting from such renewables as wind farms [15], could overload the lines. Define $\bar{\theta}_k, \bar{\theta}_m, \bar{V}_k, \bar{V}_m$ as the average values and $\hat{\theta}_k(t) := \theta_k(t) - \bar{\theta}_k, \hat{\theta}_m(t) := \theta_m(t) - \bar{\theta}_m, \tilde{V}_k(t) := V_k(t) - \bar{V}_k, \tilde{V}_m(t) := V_m(t) - \bar{V}_m$ as the fluctuating values. Under the assumption that $P_{km}(t)$ depends more on the phase angles than the bus voltages and that the transmission lines are nearly lossless, the following first order approximation is easily obtained [8]:

$$\tilde{P}_{km}(t) = B_{km}\bar{V}_k\bar{V}_m \cos(\bar{\theta}_k - \bar{\theta}_m) (\hat{\theta}_k(t) - \hat{\theta}_m(t)). \quad (1)$$

The authors are with Ming Hsieh Department of Electrical Engineering, University of Southern California, Los Angeles, CA 90089.
E-mail: {jonckhee, egrippo}@usc.edu, banirazi@gmail.com

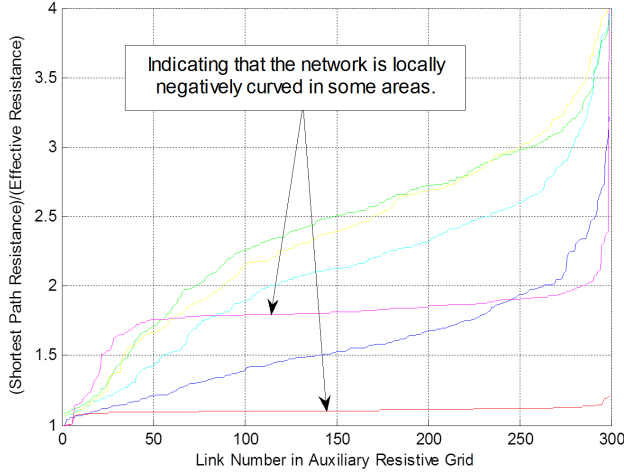


Fig. 1. A sample of five $\rho_{\text{lrp}}/\rho_{\text{eff}}$ curves for the S -graph (Eq. (4)) of the IEEE300 bus system, where flat curves close to the lower bound of 1 indicate negative curvature along the corresponding paths in accordance with the Ollivier-Ricci concept [16].

Regarding the reactive power fluctuation, on the other hand, it is assumed that $Q_{km}(t)$ depends more on the bus voltages than the phase angles. Further, assuming that the line is nearly lossless, and using the approximation $\bar{V}_k \approx \bar{V}_m \cos(\bar{\theta}_k - \bar{\theta}_m)$, which was verified on the IEEE 300 bus system [8], it follows that the first order reactive power flow approximation reads

$$\tilde{Q}_{km} = B_{km} \bar{V}_k \bar{V}_m \cos(\bar{\theta}_k - \bar{\theta}_m) \left(\frac{\tilde{V}_k(t)}{\bar{V}_k} - \frac{\tilde{V}_m(t)}{\bar{V}_m} \right). \quad (2)$$

Define the fluctuating complex power $\tilde{S}_{km}(t) = \tilde{P}_{km}(t) + j\tilde{Q}_{km}(t)$. Combining Eqs. (1)-(2) yields the approximate fluctuating complex power equations

$$\tilde{S}_{km} = B_{km} \bar{V}_k \bar{V}_m \cos(\bar{\theta}_k - \bar{\theta}_m) \underbrace{\left(\left(\tilde{\theta}_k + j \frac{\tilde{V}_k(t)}{\bar{V}_k} \right) - \left(\tilde{\theta}_m(t) + j \frac{\tilde{V}_m}{\bar{V}_m} \right) \right)}_{\tilde{E}_{km}}. \quad (3)$$

Clearly the fluctuating complex power can be viewed as a (complex) current flowing through the resistor

$$\rho_{km} = 1/B_{km} \bar{V}_k \bar{V}_m \cos(\bar{\theta}_k - \bar{\theta}_b) \quad (4)$$

subject to the complex potential difference \tilde{E}_{km} . We refer to this resistive network as S -graph.

III. CURVATURE, CENTRALITY, AND CONGESTION

A. Grid Curvature

We define curvature of an idealized infinite resistive network via the fraction, already defined in [10],

$$\lim_{\rho_{\text{lrp}}(k,m) \rightarrow \infty} \frac{\rho_{\text{lrp}}(k,m)}{\rho_{\text{eff}}(k,m)} \geq 1. \quad (5)$$

In the above, $\rho_{\text{lrp}}(k,m)$ is the resistance of the least resistive path from k to m in the network, obtained for example by the Bellman-Ford or the Dijkstra algorithm, and $\rho_{\text{eff}}(k,m)$

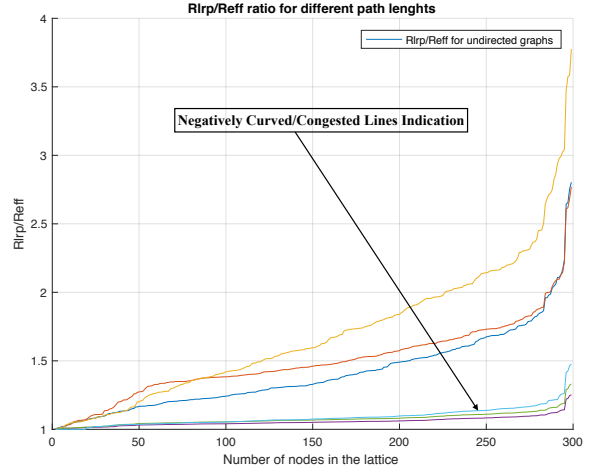


Fig. 2. Flat areas of $\rho_{\text{lrp}}/\rho_{\text{eff}}$ curves for the P -graph of the IEEE300 bus system indicating negative curvature along the corresponding paths

is the effective resistance “seen” at the port km . Precisely, inject a current I at node k and draw the same current at node m ; then, $\rho_{\text{eff}}(k,m) := (V_k - V_m)/I$, where V_k and V_m are the voltages induced at nodes k and m , resp.

Definition 1 (Negative Curvature): An infinite network is said to be negatively curved if (5) is bounded and positively curved otherwise. A finite network is said to be negatively curved if the fraction (5) is near its lower bound.

This curvature concept is specialized for power flow problems, although it has some commonalities with the Gromov [10], [11] and the Ollivier-Ricci [16] concepts. The latter is a curvature concept, *along a path* rather than at a vertex, *directly* related to transport and hence congestion.

If we construct the S -graph model (see Section II) of the IEEE300 bus network and compute the various fractions (5) for various buses, we obtain a family of curves as depicted in Fig. 1. Recall from [8] and [10] that each curve corresponds to an initial node a and plots all possible ratios $\rho_{\text{lrp}}(a,k)/\rho_{\text{eff}}(a,k)$ versus $k \neq a$. Given a bus a , the various k -buses are relabeled so that the various ratios $\rho_{\text{lrp}}(a,k)/\rho_{\text{eff}}(a,k)$ are in increasing order.

Considering $\rho_{\text{lrp}}(a,k)/\rho_{\text{eff}}(a,k) \geq 1$, the ratio could reach its lower bound, making the related curve “flat” with $\rho_{\text{lrp}}(a,k)/\rho_{\text{eff}}(a,k) \approx 1$. In this situation, most of the current (in the resistive model) or power (in the power grid) from a to k will flow along the least resistive path, hence overloading the transmission lines along that path. Geometrically, this means that the curvature is negative. From Fig. 2, it is also clear that the IEEE300 P -graph model has several overloaded lines corresponding to flat curves. More accurate inspection reveals that there are at least 15 buses with a flattening behavior along the entire grid, which is further betrayed by the consistent congestion behavior depicted in Fig. 4 (Sec. III-B).

Conversely, if $\rho_{\text{lrp}}(a,k)/\rho_{\text{eff}}(a,k)$ is monotone increasing above 1, this implies that there are many paths of a resistance slightly above ρ_{lrp} , and so the current or power will be distributed along those various paths without overloading some

specific ones. Geometrically, this means that the curvature is positive.

Going back to Fig. 2 (and Fig. 1), recall that each curve is formed by the points that represent the values of the ratio $\rho_{\text{lrp}}(a, k)/\rho_{\text{eff}}(a, k)$ for a fixed bus a and varying buses k .

Definition 2 (Critical Buses): A bus a is critical if its related $\rho_{\text{lrp}}(a, k)/\rho_{\text{eff}}(a, k)$ curve tends to be a flat line for the majority of varying buses k .

Note that various points on a $\rho_{\text{lrp}}(a, k)/\rho_{\text{eff}}(a, k)$ curve represent ratio values for different paths, named $(a, 1), (a, 2), \dots$, and so, the curve carries information about many branches, which form different paths. Therefore, the topological information extracted from a flat curve is directly related to the transmission lines connected to its corresponding bus.

Definition 3 (Critical Lines): A critical line is a transmission line connected to a critical bus.

The critical lines/buses are responsible for most of the congestion in the grid.

B. New Curvature Centrality Concept

Different graph theoretic centrality measures specialized to the power grid can be found in the literature [9], [12]–[14]. The present work, which follows in the footsteps of [8], has the unique feature that it relates *directly* to congestion (Def. 2 and Def. 3), rather than referring to a graph-theoretic feature that can be related to congestion.

Definition 4 (Centrality): The curvature centrality $\beta(a)$ of a critical bus a is the number of times the bus a appears in the “flat” paths revealed by the $\rho_{\text{lrp}}/\rho_{\text{eff}}$ diagram.

Clearly, the flat areas of the $\rho_{\text{lrp}}/\rho_{\text{eff}}$ curves are revealing that the grid/network has serious topological defect that creates high curvature centrality (hence congestion) as evidenced by Fig. 4. Unfortunately, the topology of the grid can only be changed at significant cost, so that we will have to find less costly alternatives to manipulate the curvature.

IV. CURVATURE SMOOTHING AND CURVATURE-DRIVEN OPTIMAL POWER FLOW (CD-OPF)

The importance of locating the critical areas or lines and the impact they could have on the power grid can be understood in the general context of extreme events [14]. Thus, the first step towards the development of a method that changes, or at least mitigates, the congestion pattern of a grid is to identify the problematic (congested /negative curvature) areas/buses/lines; the second step is to develop a strategy that changes this congestion trend of the grid.

This paper proposes such a strategy, which will be called *Curvature-Driven OPF*,

More specifically, this section develops the two component parts of such method. The first one (Sec. IV-A) addresses the standalone *curvature smoothing* (utilizing FACTS devices) for the DC model of the power grid; and the second one (Sec. IV-C) simultaneously smooths the curvature and reduces the overall generation cost of the grid by deploying extra *loads*, for both DC and AC models.

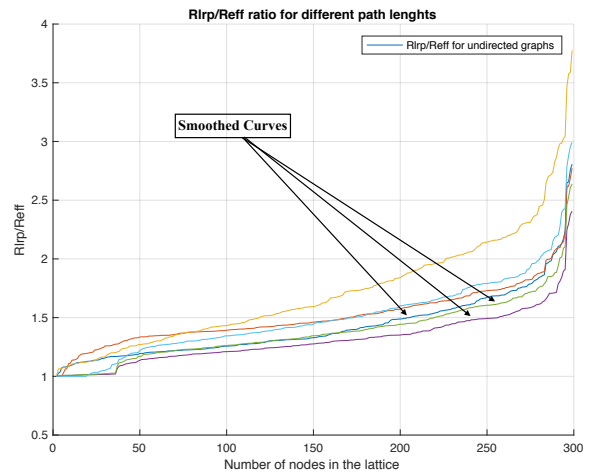


Fig. 3. Monotone increasing property of $\rho_{\text{lrp}}/\rho_{\text{eff}}$ curves for the P -graph (DC Assumptions) of the IEEE300 bus system after curvature smoothing, resulting in removal of negative curvature along the corresponding paths

A. Curvature Smoothing

The $\rho_{\text{lrp}}(k, m)/\rho_{\text{eff}}(k, m)$ technique [10] basically abstracts the power grid as a resistive network. As per equation (5) and Def. 1, changing the resistances of the resistive network model would change the curvature of the resistive network, and hence of the grid. The curvature should be changed in such a way as to generate positive curvature in those negatively curved areas prone to congestion, such as those identified by the proposed $\rho_{\text{lrp}}(k, m)/\rho_{\text{eff}}(k, m)$ tool. As seen from the DC assumptions of Sec. II, the P -graph resistive model of the grid is composed of resistors with $\rho_{k,m}$ resistances that depend only on voltages V_k, V_m and susceptances B_{km} . Though the voltages can be controlled via transformer tap changers, we leave them be unchanged for the grid voltage stability operations. Thus, we are left with the susceptance values B_{km} . While no control can be directly exercised upon the line susceptances, the apparent susceptances can be modified by, for example, FACTS series compensation to modify line impedance and static synchronous series compensator (SSSC) that connects an inductive or capacitive reactance in series with the transmission line.

The adjustment of those B_{km} susceptance values associated with the $\rho_{k,m}$ of the problematic areas/lines identified by the $\rho_{\text{lrp}}(k, m)/\rho_{\text{eff}}(k, m)$ method has been done using heuristics and the results are shown in Fig 3.

The heuristic procedure identifies the critical buses and increases the susceptance of the lines connecting those critical buses. Notice again that we defined the critical buses as the end-nodes of the critical transmission lines. Thus, by making those buses less critical, we in fact make the critical lines less prone to overload.

B. Curvature-Driven Optimal Power Flow (CD-OPF)

Once the curvature of the grid has been *smoothed* (Sec. IV-A) the second part of the procedure deploys additional loads in the neighborhood of the critical a buses so as to drain

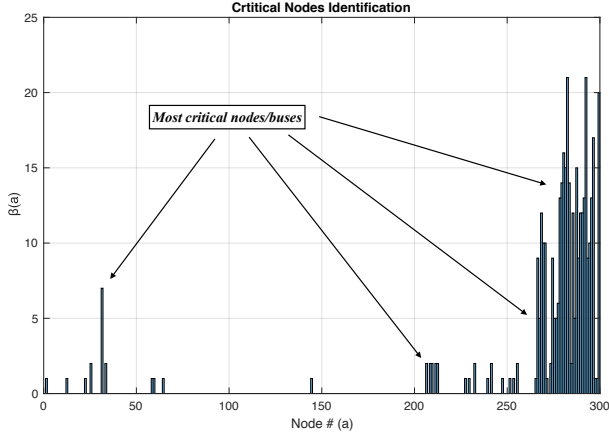


Fig. 4. Curvature centrality of critical nodes, $\beta(a)$, as per Definition 4. The height of each bar represents the number of times each critical bus appears within all critical lines.

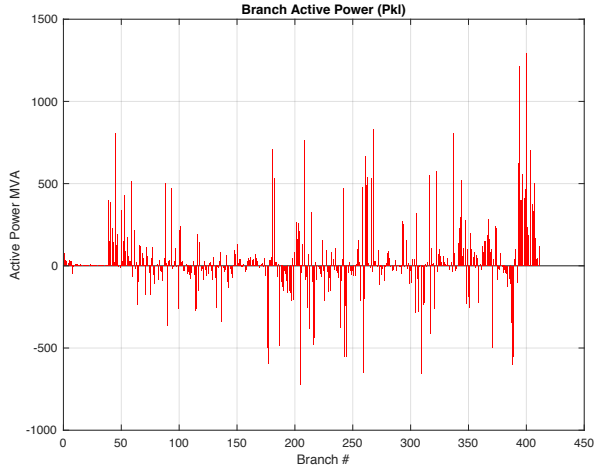


Fig. 5. Active power distribution within the IEEE300 bus system after conventional OPF (DC Assumptions)

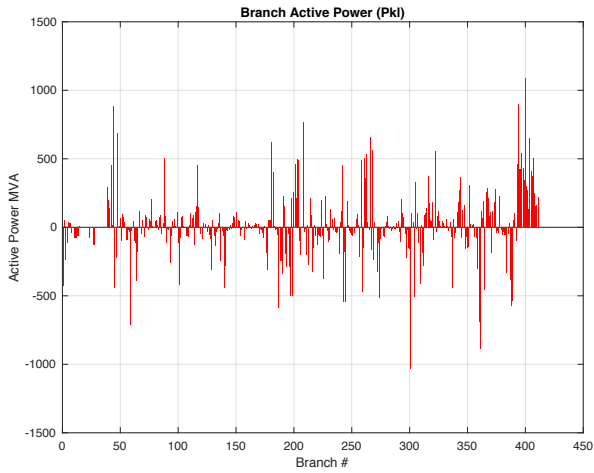


Fig. 6. Active power distribution within the IEEE300 bus system after CD-OPF (DC Assumptions)

some power away from the a 's; then the generation is re-adjusted by minimizing the overall cost of the active power generation. Clearly, this second stage of the proposed method allows energy to be stored while at the same time minimizing the overall cost of generating active power within the grid.

Recall that the critical nodes are identified via the $\rho_{\text{IRP}}(k, m)/\rho_{\text{eff}}(k, m)$ tool/plots shown in Fig. 2 and such critical nodes are more clearly shown in Fig. 4 along with their centralities. This type of plots are basically showing how many transmission lines within the grid are behaving as overloaded paths, which is captured by the ratio $\rho_{\text{IRP}}(k, m)/\rho_{\text{eff}}(k, m)$. In order to understand the identification of these particular paths, recall that the main branches of a tree are always congested, and that their $\rho_{\text{IRP}}(k, m)/\rho_{\text{eff}}(k, m)$ ratio is always equal to one, because the shortest path resistance coincides with ρ_{eff} (effective resistance) in the core branches of a tree.

As mentioned above, to carry out the second step in this *Curvature-Driven OPF* procedure, a collection of additional loads are deployed in the surrounding buses of the *critical buses* (Def. 2). The aim of these loads is to drain the excess power from the grid and store it in adequate reservoirs. Once the loads are deployed, a new set of power flow equations (incorporating the new loads) are solved by a convex optimization algorithm, with the objective of minimizing a polynomial cost function of the active power of each generator. Under the DC assumptions mentioned in Sec. II, the overall optimization problem reduces to an optimization with a degree-2 cost functional and linear constraints. Therefore, the overall optimization problem can be represented by the following nonlinear programming algorithm.

Algorithm IV.1: DC COST OPTIMIZATION (θ, P_g)

$$\begin{aligned} \min_{\theta, P_g} \quad & \sum_{k=1}^{\text{gensize}} \mathcal{C}_{\text{DC}}(P_{g,k}) \\ \text{s.t.} \quad & \begin{cases} F_{\text{DC}}(\theta, P_g) = 0 \\ \underline{\theta}_i \leq \theta_i \leq \bar{\theta}_i & i = 1, \dots, \text{bussize} \\ \underline{P}_{g,k} \leq P_{g,k} \leq \bar{P}_{g,k} & k = 1, \dots, \text{gensize} \end{cases} \end{aligned}$$

return (θ, P_g)

In the algorithm, $P_{g,k}$ stands for the active power generated by generator k , gensize is the number of generators in the grid, $x = [\theta, P_g]$ is the optimization state variable where θ is the phase angle vector carrying the buss phase angles and P_g is the vector of active powers generated by the generators; bussize is the number of buses in the grid; $\mathcal{C}_{\text{DC}}(\cdot)$ is a degree-2 cost function that weights the cost of generation of each generator k :

$$\mathcal{C}_{\text{DC}}(P_{g,k}) = \alpha_{g,k} (P_{g,k})^2 + \beta_{g,k} (P_{g,k}) + \gamma_{g,k}.$$

$F_{\text{DC}}(\cdot) = 0$ denotes the linearized power flow equations developed in Sec. II; and finally $(\underline{P}_{g,k}, \bar{P}_{g,k})$ and $(\underline{\theta}_i, \bar{\theta}_i)$ are the *min* and *max* limits for $P_{g,k}$ and θ_i , respectively.

Observe that the cost function is composed of ' gensize ' order-two polynomials that could be built up differently for

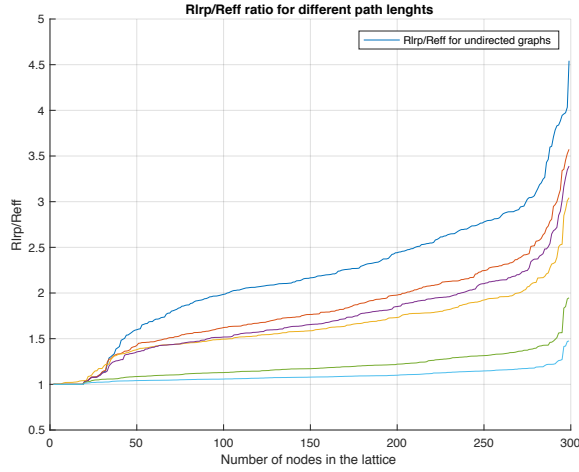


Fig. 7. ρ_{lrp}/ρ_{eff} for the DC model of the IEEE300 bus system after CD-OPF implementation

each generator; thus, we can weight (choosing $\alpha_{g,k}$, $\beta_{g,k}$ and $\gamma_{g,k}$) each generator cost differently by shaping each polynomial separately.

Fig. 5 and Fig. 6 show the active power distribution within the lines of the IEEE300 bus system *after* the implementation of the conventional OPF and the *curvature driven* OPF (CD-OPF), resp.. The simulations have been implemented within the MATPOWER environment and have been run under the DC model assumptions. As it can be seen from the simulations, the CD-OPF implementation (Fig. 6) shows a reduction of the highest active power peaks, but it does not seem to present noticeable changes with respect to the implementation of the conventional OPF (Fig. 5), although a dramatic active power cost reduction is hidden. Indeed, the CD-OPF approach utilizes an optimal set of generators that spend almost 40% less energy than the conventional OPF.

Quantitatively, the overall cost function value in each case is shown in Table I. The numbers clearly show the effectiveness of the *Curvature-Driven OPF procedure*. The total number of deployed storages were 47, all of them deployed in the surroundings of the critical buses: buses 25 to 30, 200 to 220 and buses 250 to 269 (see Fig. 4). Also, a total of 37 most critical lines were balanced so as to maximize the curvature (lines having any bus between 270 and 300 as an extreme end, see Fig. 4 and Def. 3).

TABLE I

TOTAL COST FUNCTIONS VALUES (DC MODEL WITH CONVENTIONAL OPF AND WITH CD-OPF IMPLEMENTATION)

(dollars/hr)	Total Cost Function Value
with conventional OPF	706290.00
with CD-OPF	477540.00

C. Curvature-Driven OPF under AC Assumptions

To further consolidate the curvature and the cost benefits, the CD-OPF method was investigated under a less restrictive model assumption scenario. The curvature smoothing

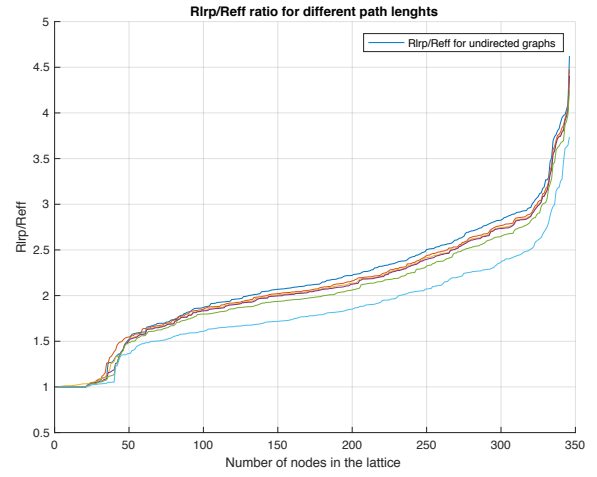


Fig. 8. ρ_{lrp}/ρ_{eff} for the Pseudo-AC model of the IEEE300 bus system after CD-OPF implementation

procedure was implemented within a *Pseudo-AC Resistive Model*, where the resistance part (R_{km}) of the B_{km} of the lines is not completely neglected. This gives an additional degree of freedom in the adjustment (using FACTS) of the susceptance B_{km} , which is now composed of X_{km} and R_{km} and somehow agrees more with the real case scenarios. As regards the cost optimization procedure, a pure AC model is utilized, which yields the following new optimization problem set up:

Algorithm IV.2: AC COST OPTIMIZATION(θ, V, P_g, Q_g)

$$\min_{\theta, V, P_g, Q_g} \sum_{k=1}^{\text{gensize}} \mathcal{C}_{AC}(P_{g,k}, Q_{g,k})$$

subject to

$$\left\{ \begin{array}{ll} F_{AC}(\theta, V, P_g, Q_g) = 0 & \\ \underline{\theta}_i \leq \theta_i \leq \bar{\theta}_i & i = 1, \dots, \text{bussize} \\ \underline{v}_i \leq v_i \leq \bar{v}_i & i = 1, \dots, \text{bussize} \\ \underline{P}_{g,k} \leq P_{g,k} \leq \bar{P}_{g,k} & k = 1, \dots, \text{gensize} \\ \underline{Q}_{g,k} \leq Q_{g,k} \leq \bar{Q}_{g,k} & k = 1, \dots, \text{gensize} \end{array} \right.$$

return (θ, V, P_g, Q_g)

where the added variables (compared to the DC model) are the $Q_{g,k}$'s, which stand for reactive powers generated, and the v_i 's, which stand for the bus voltages; the augmented state vector $x = [\theta, v, P_g, Q_g]$ now becomes the new optimization variable; and $F_{AC}(\cdot) = 0$ represents the dynamic of the AC power flow. Observe now that the cost function $\mathcal{C}_{AC}(\cdot)$ is a degree-2 polynomial on $P_{g,k}$ and $Q_{g,k}$:

$$\mathcal{C}_{AC}(P_{g,k}, Q_{g,k}) = \alpha_{g,k}(P_{g,k})^2 + \beta_{g,k}(P_{g,k}) + \delta_{g,k}(Q_{g,k})^2 + \psi_{g,k}(Q_{g,k}) + \gamma_{g,k} \quad (6)$$

Not too unsurprisingly, the increased complexity and dimensionality of the *Pseudo-AC / AC model* allows for a wider range of adjustment of the curvature and a more

cost-effective deployment of the additional loads to drain power away from the congestion areas. These results can be appreciated by comparing Fig. 7, Fig. 8, and Table II (against Table I).

TABLE II

TOTAL COST FUNCTIONS VALUES (AC MODEL WITH CONVENTIONAL OPF AND WITH CD-OPF IMPLEMENTATION)

(dollars/hr)	Cost Function Value
with conventional OPF	719730.00
with CD-OPF	492280.00

Clearly a better smoothing of the lines was achieved and the cost reduction, although it is not as big as in the *DC* case, still yields outstanding reduction results. The location of the deployed loads and the adjusted (load balancing) lines were the same as the ones in the *DC* case.

The overall content of this section is summarized in Table III.

TABLE III

CURVATURE SMOOTHING AND CURVATURE-DRIVEN OPF "MAIN STEPS" (recall that critical buses and critical lines are defined in Def. 2 and Def. 3, resp.)

Curvature Smoothing (IV-A)	identify critical buses
	adjust B's (w / FACTS) of critical lines
Curvature Driven OPF (IV-B and IV-C)	identify critical buses
	adjust B's (w / FACTS) of critical lines
	deploy loads around critical buses
	cost optimization { DC Algorithm IV.1 AC Algorithm IV.2

V. LINE RATING CONSIDERATIONS

Until this point, no *line rating* has been considered in order to highlight the power flow that the generation and demand impose upon the grid given its current topology. Thus, the active power flow through the branches has been allowed to exceed its limits. To account for the capacity of the lines, usually determined by the thermal rating [21], [23], [24], we introduce a *utilization factor* for each line:

Definition 5 (DC Utilization Factor): The *utilization factor* for the branch (k, m) under *DC model assumptions* is defined as

$$\mu_{DC(k,m)} = P_{(k,m)} / LC_{(k,m)},$$

where $LC_{(k,m)}$ stands for *line capacity*, the maximum active power allowed (in MW) through the branch (k, m) .

Definition 6 (AC Utilization Factor): The *utilization factor* for the branch (k, m) under *AC model assumptions* is defined as

$$\mu_{AC(k,m)} = \sqrt{P_{(k,m)}^2 + P_{(m,k)}^2} / LC_{(k,m)}.$$

The impact of adding the line limitation constraints

$$\mu_{DC(k,m)} \leq 1, \quad \mu_{AC(k,m)} \leq 1,$$

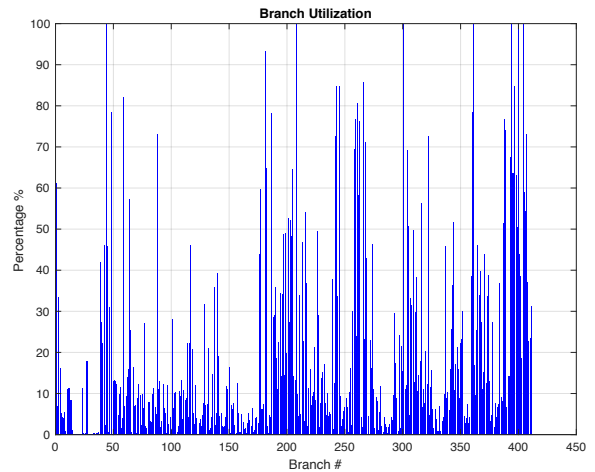


Fig. 9. Utilization Factor (μ_{DC}) for the DC model of the IEEE300 bus system with CD-OPF and a 700 MW active power constraint

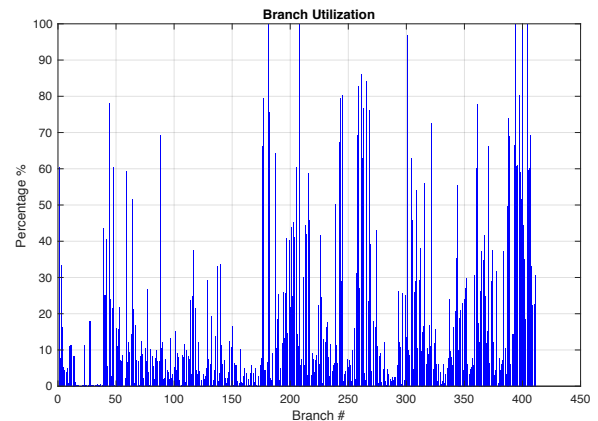


Fig. 10. Utilization Factor (μ_{AC}) for the AC model of the IEEE300 bus system with CD-OPF and a 700 MW active power constraint

in the DC and AC Curvature-Driven OPF is barely noticeable in the overall final cost function values for a line limit of $LC_{(k,m)} = 700\text{MW}$, although it underlines an important advantage within the complete method: the CD-OPF scheme is now able to handle realistic line limits.

Fig. 9 and Fig. 10 show a line utilization histogram (in percentage) for the IEEE 300 bus system with a line rating of 700 MW (on the active power of the branches) under both DC and AC analysis.

The increase of *thermal stress* due to variable weather or other conditions [19], [20], [23], [24] could easily trigger a line overloading that might end up in a blackout (e.g., 1996 Western North America blackout [21]). As another scenario, when a major line trips, power is rerouted along other lines that may not have been designed to carry such an amount of power and hence are likely to be overloaded and trip, leading to a chain reaction effect [22]. Thus, a real time power flow calculation which includes a DLR (Dynamic Line Rating [23]) could certainly help to assess power grid functionality.

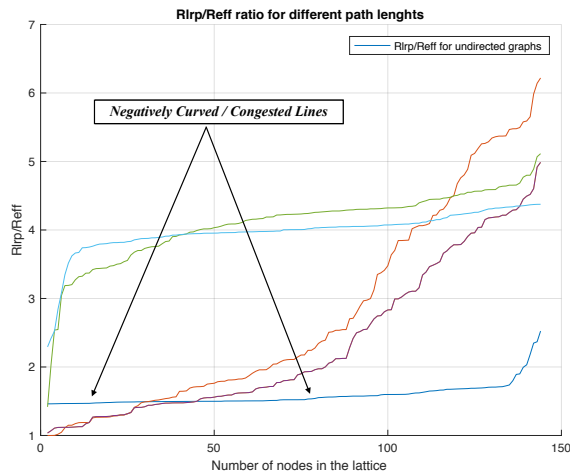


Fig. 11. Flat areas of ρ_{lRp}/ρ_{eff} curves for the P -graph of the IEEE145 bus system indicating negative curvature along the corresponding path

VI. DISCUSSION AND CONCLUSION

Although the DC model, or any other model for that matter, helps to make quick conclusions on the grid behavior, there is really an important difference between the power grid and its models. As is known, the power grid is a dynamic nonlinear system acting at different time-scales, some aspects of which, like the fractal behavior of the PMU signals, are still poorly understood [17], [18]. Since it is still very unclear how the fractional dynamics betrayed by the PMU signal analysis can be used for enhanced modeling, here we have limited ourselves to utilize the AC model for combined curvature smoothing and generation cost reduction. The new AC optimization procedure has drastically reduced the overall cost of the generation necessary to sustain the power flow relative to the simpler models. The line rating considerations have opened a door for the future inclusion of thermal rating calculations. Finally, as a future step of this work, an optimization procedure that includes the hitherto unknown dynamical effects revealed by the data driven approach of [17], [18] could further enhance the combined curvature smoothing/cost reduction—for real grids.

REFERENCES

- [1] Nurul Idayu Yusoff, Abdullah Asuhaimi Mohd Zin, and Azhar Bin Khairuddin. Congestion Management in Power System: A Review. In *2017 3rd International Conference on Power Generation Systems and Renewable Energy Technologies (PGSRET)*, Johor Bahru, Malaysia, April 4-6 2017.
- [2] A. Pillay, S. Prabhakar Karthikeyan, and D. P. Kothari. Congestion Management in Power System: A Review. In *International Journal of Electrical Power and Energy Systems*, vol. 70, pp. 83-90, 2015.
- [3] K.Vijayakumar. Optimal Location of FACTS Devices for Congestion Management in Deregulated Power Systems. In *International Journal of Computer Applications*, Volume 16 No.6, February 2011.
- [4] Hiren Patel and Ravikumar Paliwal. Congestion Management in Deregulated Power Systems Using FACTS Devices. In *International Journal of Advances in Engineering and Technology*, April 2015
- [5] Vijaya Margaret and K Uma Rao. Demand Response for Residential Loads using Artificial Bee Colony Algorithm to Minimize Energy Cost. In *TENCON 2015 - 2015 IEEE Region 10 Conference*, Macao, China, Nov 1-4 2015

- [6] Insoon Yang and Asuman E. Ozdaglar. Reducing Electricity Price Volatility via Stochastic Storage Control. In *2016 American Control Conference (ACC)*, Boston, MA, USA, July 6-8 2016.
- [7] Junjie Qin, Insoon Yang and Ram Rajagopal. Submodularity of Energy Storage Placement in Power Networks. In *2016 IEEE 55th Conference on Decision and Control (CDC)*, Las Vegas, NV, USA, Dec. 12- 14 2016.
- [8] R. Banirazi and E. Jonckheere. Geometry of power flow in negatively curved power grids. In *49th IEEE Conference on Decision and Control (CDC)*, pages 6259–6264, Atlanta, GA, December 15-17 2010.
- [9] Ulrik Brandes and Daniel Fleischer. Centrality measures based on current flow. In *Proc. 22nd Symp. Theoretical Aspects of Computer Sciences*, volume 3404/2005 of *Lecture Notes in Computer Science*, pages 533–544. Springer Berlin / Heidelberg, 2005.
- [10] E. Grippo and E. Jonckheere. Effective resistance criterion for negative curvature: application to congestion control. In *2016 IEEE Conference on Control Applications (CCA), Part of 2016 IEEE Multi-Conference on Systems and Control*, pages 129–136, Buenos Aires, Argentina, Sept. 19-22 2016.
- [11] M. Gromov. Asymptotic invariants of infinite groups. In M. A. Roller and G. Niblo, editors, *Geometric Group Theory: Proceedings of the Symposium Held in Sussex, 1991*. Cambridge University Press, 1993.
- [12] Paul Hines and Seth Blumsack. A centrality measure for electrical networks. In *HICSS '08: Proceedings of the Proceedings of the 41st Annual Hawaii International Conference on System Sciences*, page 185, Washington, DC, USA, 2008. IEEE Computer Society.
- [13] Zhifang Wang, Anna Scaglione and Robert J. Thomas. Electrical Centrality Measures for Electric Power Grid Vulnerability Analysis. In *49th IEEE Conference on Decision and Control*, Hilton Atlanta Hotel, Atlanta, GA, USA, December 15-17, 2010.
- [14] Ali Pinar, Sandip Roy and Bernie Lesieutre. Power System Extreme Event Detection: The Vulnerability Frontier. In *HICSS '08: Proceedings of the 41st Annual Hawaii International Conference on System Sciences*, page 184, Hawaii, HI, USA, 2008.
- [15] Joaquin Mur-Amada and Jess Salln-Arasanz. Power fluctuation in a wind farm compared to single turbine. In Gesche Krause, editor, *From turbine to wind farms—Technical requirements and spin-off products*, chapter 6, pages 101–132. Intech, April 2011. ISBN 978-953-307-237-1; DOI: 10.5772/15957.
- [16] Y. Ollivier. Ricci curvature on Markov chains on metric spaces. arXiv:0701886v4 [math.PR] 30 Jul 2007, 2007.
- [17] L. Shalalfeh, P. Bogdan, and E. Jonckheere. Evidence of long range-dependence in power grid. In *Power and Energy Society General Meeting (PESGM)*, Boston, MA, July 2016. Available at <http://eudoxus2.usc.edu>.
- [18] L. Shalalfeh, P. Bogdan, and E. Jonckheere. Kendall's tau of frequency Hurst exponent as blackout proximity margin. In *IEEE International Conference on Smart Grid Communications*, Sydney, Australia, November 06-09 2016. 978-1-5090-4075-9/16; available at <http://eudoxus2.usc.edu>.
- [19] CIGRE Working Group B2.43. Guide for Thermal Ratings Calculation of Overhead Lines. In *IEEE Transactions on Power Delivery*, December 2014
- [20] IEEE Std. IEEE Standard for Calculating the Current-Temperature Relationship of Bare Overhead Conductors. page 738, 2012
- [21] T. Morgan. Effect of Elevated Temperature Operation on the Tensile Strength of Overhead Conductor. In *IEEE Transactions on Power Delivery*, Vol. 11, No. 1, pages. 345-51, January 1996.
- [22] Federal Energy Regulatory Commission and the North American Electric Reliability Corporation. Arizona-Southern California Outages on September 8, 2011. Causes and Recommendations. April, 2012.
- [23] J. Heckenbergerova and J. Hosek. Dynamic thermal rating of power transmission lines related to wind energy integration. In *11th International Conference on Environment and Electrical Engineering (EEEIC), Venice, Italy, 18-25 May 2012*. (DOI: 10.1109/EEEIC.2012.6221484)
- [24] H. Wan and J.D. McCalley. Increasing thermal rating by risk analysis. In *IEEE Transactions on Power Systems*, volume 14, number 3, pp. 815 - 828, Aug. 1999.